Journal of Alloys and Compounds 509 (2011) 602–608

Contents lists available at ScienceDirect

Journal of Alloys and Compounds

journal homepage: www.elsevier.com/locate/jallcom

Phase diagram and thermodynamic properties of the system As–Te–I

Z.S. Aliev[a], D.M. Babanly[a], M.B. Babanly[a,*], A.V. Shevelkov[b,**], I.R. Amiraslanov[c]

[a] Baku State University, General and Inorganic Chemistry Department, Baku, Azerbaijan
[b] Moscow Lomonosov State University, Chemistry Department, Leninskie Gory 1-3, Moscow 119991, Russia
[c] Institute of Physics, Azerbaijan National Academy of Science, Baku, Azerbaijan

ARTICLE INFO

Article history:
Received 16 July 2010
Received in revised form
22 September 2010
Accepted 28 September 2010
Available online 8 October 2010

Keywords:
Phase diagrams
Arsenic
Thermodynamic properties
Electro-motive force

ABSTRACT

The As–Te–I system has been investigated primarily by means of DTA, XRD analyses and EMF measurements with an arsenic electrode. The T–x diagram of the binary As–I system was accurately redefined and its phase diagram was constructed. A projection of the liquidus surface, an isothermal section at 300 K, and a series of polythermal sections of the phase diagram were constructed. The previously reported ternary compounds As_5Te_7I, $As_4Te_5I_2$ and $As_8Te_7I_5$ were confirmed to be equilibrium phases; the positions of phase areas with their participation were established. Areas of primary crystallization of phases, types and coordinates of the invariant equilibria on the T–x–y diagram were determined. From the X-ray powder diffraction (XRD) analysis, the crystallographic parameters of $As_4Te_5I_2$ and $As_8Te_7I_5$ were determined. From the EMF measurements, the partial molar functions of arsenic ($\Delta\bar{G}$, $\Delta\bar{H}$, $\Delta\bar{S}$) as well as standard integral thermodynamic functions of ternary compounds were calculated.

1. Introduction

For many years there has been an interest in the vast family of arsenic, antimony and bismuth chalcogen–halides. These compounds exhibit properties that make them a good base for creating various functional materials, including ferro- and piezoelectrics, piezoelastics, thermoelectrics, and photoconductors [1–3]. The preparative routes to these compounds, and especially to their large crystals, are not always straightforward; in many cases they require the knowledge of the respective phase diagrams.

The ternary As–Te–I system was investigated along the polythermal sections As_2Te_3–AsI_3, AsI_3–TeI_4, and in the composition area As–As_2Te_3–AsI_3 [4–6]. The AsI_3–TeI_4 system was reported to be of a simple eutectic type [4]. The eutectic composition has the melting point of 405 K at 5 mol.% TeI_4. According to the literature [5], the section As_2Te_3–AsI_3 includes the only compound $As_4Te_5I_2$ that melts congruently at 563 K, whereas the eutectic compositions were found to be 23 and 92 mol.% AsI_3 at the temperatures 553 and 403 K, respectively. In the system there are solid solubility ranges on the base of both As_2Te_3 and $As_4Te_5I_2$. According to the literature [6], the composition area As–As_2Te_3–AsI_3 of the system As–Te–I contains the ternary compounds $As_8Te_7I_5$. The phase diagram of the system As–$As_4Te_5I_2$ was constructed from the DTA results. It was established that this section is quasi-binary and characterized by monotectic and eutectic equilibriums. The eutectic composition has the melting point of 553 K at 87.5 mol.% $As_4Te_5I_2$. The monotectic temperature is achieved at 583 K, and the immiscibility area ranges from 2 to 70 mol.% $As_4Te_5I_2$. The projection of the liquidus surface of subsystem As–As_2Te_3–AsI_3 consists of five areas of the primary crystallization fields (As, As_2Te_3, AsI_3, $As_4Te_5I_2$ and $As_8Te_7I_5$). The area of the primary crystallization of arsenic occupies up to 95% of the As–As_2Te_3–AsI_3 triangle area. There is a wide immiscibility area in the subsystem. The comparative analysis of the system As–$As_4Te_5I_2$ and the liquidus surface shows that the borders of the immiscibility area in the subsystem are shown incorrectly. Thus, according to [6], the immiscibility area on the liquidus surface ranges from 21 to 95 mol.% $As_4Te_5I_2$. Also, eutectic and monotectic equilibriums of the system As–$As_4Te_5I_2$ are not shown on the projection of the liquidus surface.

Three phases are reported to exist in the system As–Te–I; they are $As_4Te_5I_2$, $As_8Te_7I_5$, and As_5Te_7I. All three compounds possess different structures. The crystal structure of As_5Te_7I is well-explored [7,8]. It crystallizes monoclinically with the following lattice parameters: $a = 14.5520$ Å, $b = 4.0335$ Å, $c = 13.8440$ Å, $\beta = 112^\circ$, $z = 2$, and the space group either Cm or $C2/m$, depending on whether the Te/I joint occupancy of same crystallographic positions allowed or not. In this structure, the As–Te–I slabs run along the b axis in such a way that the As atoms inside the slab are surrounded by six Te and/or I atoms while the As atoms at the sides of the slab are three-coordinated. This structure forms its own structure type, though some similarity to the crystal structure of $Bi_{11}Se_9Cl_{12}$ can be noticed [9,10]. Less is known about the

* Corresponding author at: Z. Khalilov Str. 23, Baku, AZ 1148, Azerbaijan.
** Corresponding author.
E-mail addresses: babanly_mb@rambler.ru (M.B. Babanly), shev@inorg.chem.msu.ru (A.V. Shevelkov).

0925-8388/$ – see front matter © 2010 Elsevier B.V. All rights reserved.
doi:10.1016/j.jallcom.2010.09.198

crystal structure of two other compounds. $As_4Te_5I_2$ is reported to have the face-centered cubic structure with the unit cell parameter of 5.7825 Å [6]. Arguably, it crystallizes with the defect zinc-blend type. No crystallographic data are available for $As_8Te_7I_5$ save for the XRD pattern [6].

In our previous report some results on the subsystem As_2Te_3–AsI_3–Te [11] were presented. The phase diagrams of the quasi-binary systems As_2Te_3–AsI_3 and AsI_3–Te were constructed. It was shown that below the solidus this subsystem consists of three three-phase areas AsI_3–$As_4Te_5I_2$–Te, $As_4Te_5I_2$–As_5Te_7I–Te and As_2Te_3–As_5Te_7I–Te.

In this work, we report the results of the complete investigation of phase equilibriums in the As–Te–I system and of thermodynamic properties of the three ternary compounds in this system, As_5Te_7I, $As_4Te_5I_2$, and $As_8Te_7I_5$. Similar reports on the investigation of the Sb(Bi)–Te–I systems have been already presented in the literature [12–14].

2. Experimental

As_2Te_3, AsI_3, TeI_4, TeI, TeI_4, As_5Te_7I, $As_4Te_5I_2$, and $As_8Te_7I_5$ were synthesized from elements of high purity grade in evacuated ($\sim 10^{-2}$ Pa) sealed silica ampoules according to the following schemes. As_2Te_3 was prepared by a one-step annealing of the stoichiometric mixture of the elements at 700 K, which is above the melting point of As_2Te_3 (654 K), followed by cooling with the furnace. For the preparation of AsI_3, TeI_4, TeI, TeI_4, As_5Te_7I, $As_4Te_5I_2$, and $As_8Te_7I_5$, the specially designed method was used taking into account high volatility of iodine. The synthesis was performed in the inclined three-zone furnace, with two hot zones kept at 410–630 K, whereas the temperature of the cold zone was about 400 K. After the main portion of iodine reacted at about 470 K, the ampoules were relocated such that the products melted at 550–630 K. The melts were stirred at these temperatures and then cooled with the furnace.

Most of the samples, having masses of 0.5 g, were pre-prepared from the above mentioned binary and ternary compounds. After determining the solidus temperatures, the sintering temperatures were adjusted to be 20–30 K below the solidus. Subsequently, they were annealed for 800–1000 h at 500 K within the As–As_2Te_3–$As_8Te_7I_5$ field and at 380 K for the other fields.

X-ray powder diffraction and differential thermal analysis were used to analyze the samples. The XRD analysis was performed on a Bruker D8 ADVANCE diffractometer with Cu-Kα radiation. The lattice parameters were refined using the Topas V3.0 software. For the DTA measurements, the NTR-72 pyrometer equipped with two chromel–alumel thermocouples was used.

For the electro-motive force (EMF) measurements, the following concentration chains were used:

$$(-)\ \mathrm{As(solid)/glycerin + KI + AsI_3/(As{-}Te{-}I)(solid)}(+) \quad (1)$$

In the chains of type (1), "metallic" arsenic was the left (negative) electrode, while equilibrium alloys of the As–Te–I system were exploited as right (positive) electrodes. Saturated glycerin solution of KI with the addition of 0.1 mass% of AsI_3 was used as the electrolyte. EMF was measured by the compensation method in the temperature range of 300–400 K, with the accuracy of the temperature control being 0.2 K. In each experiment the first reading was performed after approximately 30 h after the start of the experiment, and then 4–5 h after reaching the desired temperature, which ensures the achievement of equilibrium.

3. Results and discussion

3.1. Phase relationship in the system As–Te–I

3.1.1. The As–I phase diagram

Inspection of the DTA data for the As–As_2I_4–$As_8I_7I_5$ compositional field showed that our results disagree with the As–I phase diagram reported in the literature [15]. Consequently, we undertook the complete study of this part of the As–Te–I system. That enabled us to build its T–x diagram (Fig. 1), which shows substantial differences from that reported previously [15], especially in the As–AsI_3 subsystem. According to Ref. 15, the As–I system is characterized by monotectic and eutectic equilibriums. Two compounds were reported to be present in this system, AsI_3 that melts congruently at 414 K and As_2I_4 forming by the syntactic reaction at 408 K, whereas the eutectic compositions were found to be 20, 70 and 86 at.% I at temperatures 393, 394 and 346 K, respectively. At

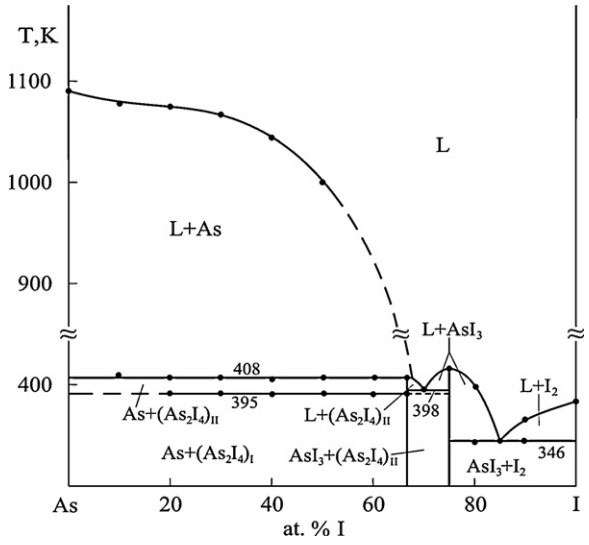

Fig. 1. Phase diagram of the As–I system.

the monotectic temperature (408 K), the immiscibility area ranges from 25 to 69.5 at.% of I.

According to our data, the monotectic equilibrium is not observed, whereas As_2I_4 decomposes by the peritectic reaction at 408 K. On the DTA curves of the As–AsI_3 samples weak peaks at 395 K adjoining peaks at 408 K were observed. It is possible that these peaks appear according to the solid state phase transition of As_2I_4 (Fig. 1). The eutectic composition between AsI_3 and As_2I_4 has the melting point of 398 K at 70 at.% I.

The combined analysis of all our experimental data and the results found in the literature on the equilibria in the As–Te and Te–I system [16] enabled us to construct the self-consistent diagram of the phase equilibria in the As–Te–I system.

3.1.2. The quasi-binary sections

The section As_2Te_3–AsI_3 is shown in Fig. 2. The compounds As_5Te_7I and $As_4Te_5I_2$ melt incongruently at 620 and 605 K, respec-

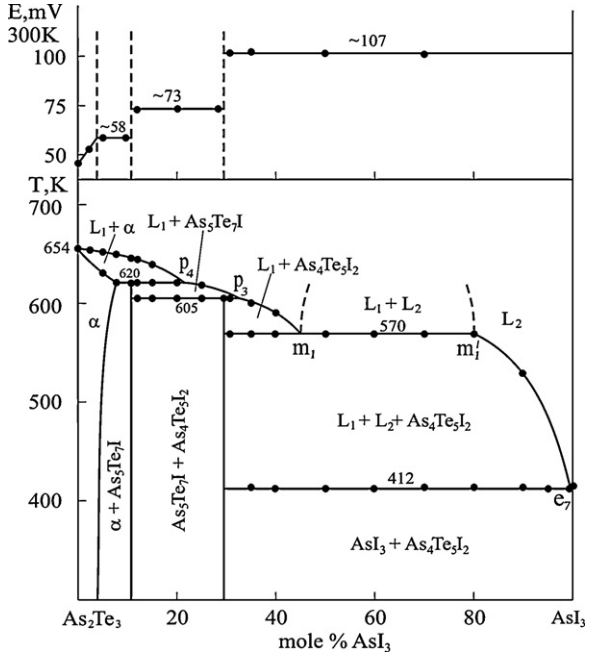

Fig. 2. T–x (bottom) and E–x (top) diagrams of the AsI_3–As_2Te_3 system.

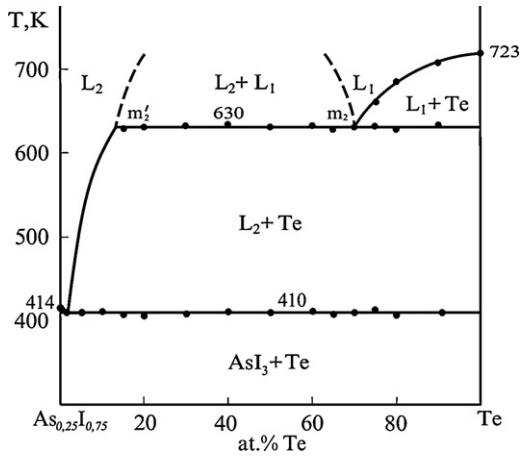

Fig. 3. Phase diagram of the $As_{0.25}I_{0.75}$–Te system.

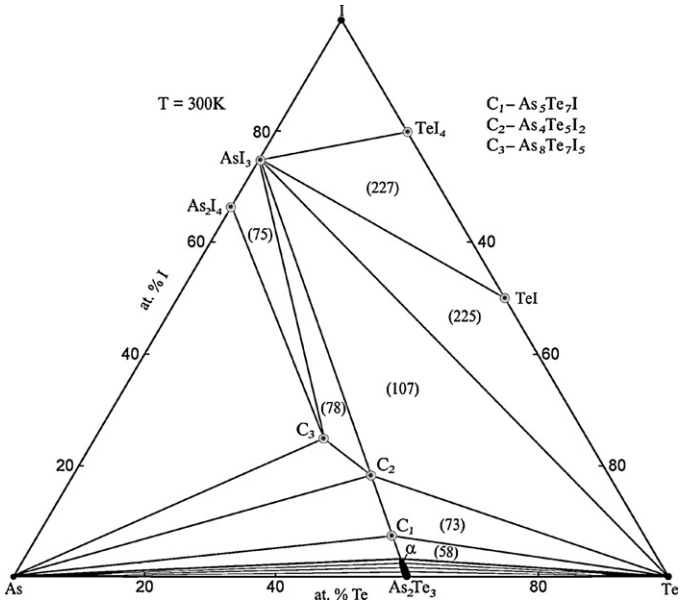

Fig. 4. Isothermal section at 300 K of the phase diagram of the system As–Te–I. The EMF values (mV) of the concentration chains of type (1) in some phase areas are indicated in parenthesis.

tively. Solid solubility based on As_2Te_3 is observed. At the peritectic temperature this area ranges from 0 to 8 mol.% of AsI_3. We did not observe appreciable solid solubility based on $As_4Te_5I_2$. This system is characterized by the monotectic ($m_1m'_1$, 570 K) and eutectic (degenerate, e_7, 412 K) equilibriums in the $As_4Te_5I_2$–AsI_3 subsystem. At the monotectic temperature, the immiscibility field ranges from 45 to 80 mol.% of AsI_3. These results do not agree with those reported elsewhere [5]. The isothermal curve of E–x at 300 K

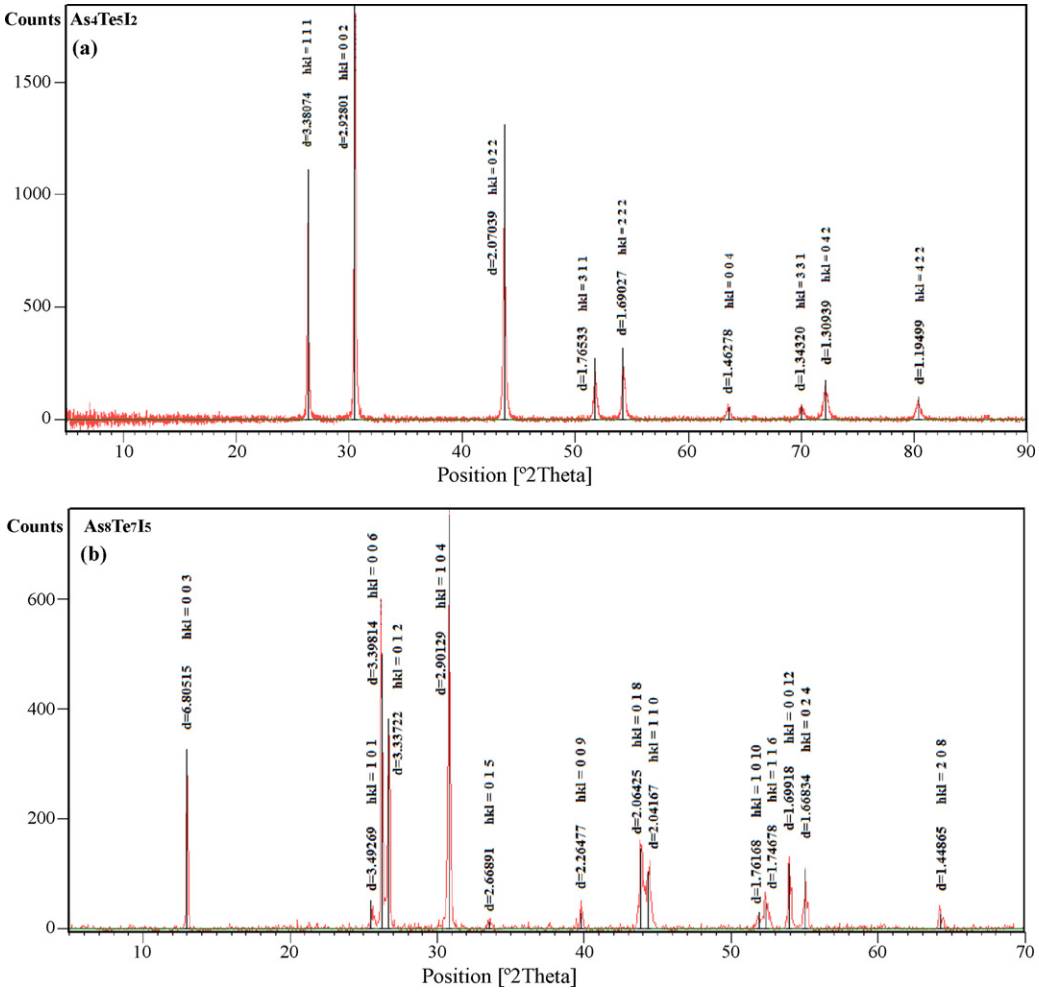

Fig. 5. The XRD patterns of $As_4Te_5I_2$ (a) and $As_8Te_7I_5$ (b) compounds.

consists of three horizontal straights with the EMF values of 58, 73 and 107 mV, which step-wisely pass from one to another at the stoichiometric compositions of $As_4Te_5I_2$ and $As_4Te_5I_2$ clearly fixing a quality changing of phase compositions of alloys (Fig. 2b). In the 0–5 mol.% As_2Te_3 the E–x curve changes continuously and this proves the existence of the solid solution based on As_2Te_3.

The section $As_{0.25}I_{0.75}$–$Te_{0.2}I_{0.8}$ is quasi-binary and relates to the simple eutectic type. The eutectic composition (e_9) lies at 5 at. % TeI_4 and 405 K, which is in agreement with that reported in Ref 4.

The section $As_{0.25}I_{0.75}$ (Fig. 3) is quasi-binary and characterized by the monotectic (m_2m_2', 630 K) and eutectic equilibriums (e_8, 410 K). The eutectic point is degenerated nearest of AsI_3. At the monotectic temperature, the immiscibility field ranges from 13 to 70 at.% of Te.

3.1.3. The isothermal section of the As–Te–I ternary system at 300 K

The isothermal section of the As–Te–I ternary system at 300 K (Fig. 4) was determined from the results of powder XRD and EMF methods. There are twelve three-phase and two two-phase regions (α + As and α + Te) in this system. The isothermal section confirms the formation of ternary compounds As_5Te_7I, $As_4Te_5I_2$ and $As_8Te_7I_5$. Fig. 4 shows that AsI_3, being the more thermodynamically stable compound of the system, has the critical influence on the distribution of the phase areas in subsolidus. This compound forms connod lines with tellurium, tellurium iodides (TeI_4 and TeI), and also with ternary compounds $As_8Te_7I_5$ and $As_4Te_5I_2$.

The EMF method allows to clearly differentiating these areas. Fig. 2 shows the values of the EMF (mV) chains of the mode (1) in certain phase areas of the system As–Te–I at 300 K. The measurements show that under specified temperature, in the range of each of three-phase areas, the EMF has a strict constant value which is independent of the general composition of alloys, but at transition from one three-phase area to another it is changed jump-like.

From the X-ray powder diffraction analysis, the lattice parameters of the $As_4Te_5I_2$ and $As_8Te_7I_5$ were determined. The XRD patterns of $As_4Te_5I_2$ and $As_8Te_7I_5$ are shown in Fig. 5. It is confirmed that $As_4Te_5I_2$ crystallizes in the face-centered cubic structure with the unit cell parameter $a = 5.854(1)$ Å, which is in a good agreement with the literature data [6]. The XRD pattern of $As_8Te_7I_5$ was indexed in the trigonal unit cell with the lattice constants $a = 4.075(3)$ Å, $c = 20.36(1)$ Å. No extra systematic conditions were observed. The crystal structure of $As_8Te_7I_5$ requires further investigation, however, based on the lattice constants and symmetry it is possible to propose a similarity with bismuth telluride-halides, which crystallize in trigonal space groups with the a parameter slightly exceeding 4 Å [17].

3.1.4. The liquidus surface of the As–Te–I system

The liquidus surface of the As–Te–I system (Fig. 6) consists of eleven fields corresponding to primary crystallization of elementary components as well as binary and ternary compounds. The fields of the primary crystallization of arsenic, tellurium and TeI_4 are very large and occupy up to 90% of the total area of the As–Te–I triangle. The crystallization of ternary compounds from liquid phase takes place in the narrow composition range along the quasi-binary system As_2Te_3–AsI_3. Our results show that the phase C_3 does not belong to any sections and its crystallization from stoichiometric liquid is multistage. Firstly, arsenic crystallizes from the liquid phase; secondly, arsenic and C_2 jointly crystallize; and thirdly, the phase C_3 forms by the L + As + C_2 ↔ C_3 peritectic reaction (Fig. 6, Table 1, point P_1). The fields of the primary crystallization of As_2I_4, AsI_3 and elementary iodine are very narrow along the binary system As–I.

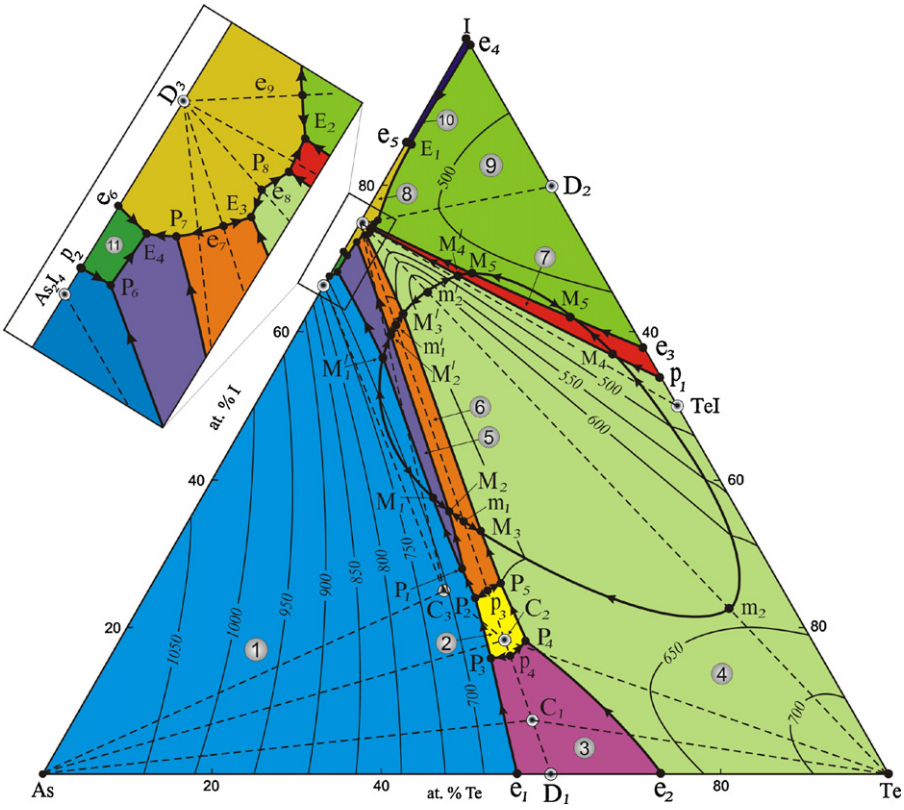

Fig. 6. Projection of the liquidus surface of the As–Te–I system. Primary crystallization fields are shown: 1, As; 2, As_5Te_7I; 3, α; 4, Te; 5, $As_8Te_7I_5$; 6, $As_4Te_5I_2$; 7, TeI; 8, AsI_3; 9, TeI_4; 10, I_2; 11, As_2I_4.

Table 1
Nonvariant equilibria in the As–Te–I system.

Point on Fig. 6	Equilibrium	Composition (at.%)		T (K)
		Te	I	
D_1	$L \leftrightarrow \alpha$	60	–	654
D_2	$L \leftrightarrow TeI_4$	20	80	553
D_3	$L \leftrightarrow AsI_3$	–	75	414
e_1	$L \leftrightarrow As \pm \alpha$	56	–	653
e_2	$L \leftrightarrow Te \pm \alpha$	73	–	636
e_3	$L \pm TeI_4 \pm TeI$	42	58	456
e_4^*	$L \leftrightarrow I_2 \pm TeI_4$	<1	>99	386
e_5	$L \leftrightarrow AsI_3 \pm I_2$	–	86	346
e_6	$L \leftrightarrow As_2I_4 \pm AsI_3$	–	71	398
e_7^*	$L \leftrightarrow AsI_3 \pm As_4Te_5I_2$	<2	~74	412
e_8^*	$L \leftrightarrow AsI_3 \pm Te$	<2	~74	410
e_9^*	$L \leftrightarrow AsI_3 \pm TeI_4$	2	~76	405
E_1^*	$L \leftrightarrow AsI_3 \pm TeI_4 \pm I_2$	<1	86	344
E_2^*	$L \leftrightarrow AsI_3 + TeI_4 \pm TeI$	<2	~75	400
E_3^*	$L \leftrightarrow AsI_3 \pm As_4Te_5I_2 \pm Te$	<2	~74	408
E_4^*	$L \leftrightarrow AsI_3 \pm As_8Te_7I_5 \pm As_2I_4$	<1	~70	395
p_1	$L \pm Te \leftrightarrow TeI$	46	54	458
p_2	$L \pm As \leftrightarrow As_2I_4$	–	68	408
p_3	$L \pm As_5Te_7I \leftrightarrow As_4Te_5I_2$	40	25	605
p_4	$L + \alpha \leftrightarrow As_5Te_7I$	47	16	620
P_1	$L \pm As \pm As_4Te_5I_2 \leftrightarrow As_8Te_7I_5$	36	28	580
P_2	$L \pm As_5Te_7I \leftrightarrow As_4Te_5I_2 \pm As$	39	24	600
P_3	$L \pm \alpha \leftrightarrow As_5Te_7I \pm As$	45	16	615
P_4	$L \pm \alpha \leftrightarrow As_5Te_7I \pm Te$	48	18	610
P_5	$L + As_5Te_7I \leftrightarrow As_4Te_5I_2 \pm As$	41	26	600
P_6^*	$L \pm As \leftrightarrow As_2I_4 \pm As_8Te_7I_5$	<1	~67	405
P_7^*	$L \pm As_4Te_5I_2 \leftrightarrow AsI_3 \pm As_8Te_7I_s$	<1	~71	400
P_8^*	$L \pm Te \leftrightarrow AsI_3 \pm TeI$	<2	~74	405
$m_1(m_1')$	$L_1 \leftrightarrow L_2 \pm As_4Te_5I_2$	32(11)	34(61)	570
$m_2(m_2')$	$L_1 \leftrightarrow L_2 \pm Te$	70(13)	22.5(66)	630
$M_1(M_1')$	$L_1 \pm As \leftrightarrow L_2 \pm As_8Te_7I_5$	27(12)	38(57)	550
$M_2(M_2')$	$L_1 \pm \leftrightarrow L_2 \pm As_4Te_5I_2 + As_8Te_7I_5$	30(11)	36(60)	535
$M_3(M_3')$	$L_1 \leftrightarrow L_2 \pm As_4Te_5I_2 \pm Te$	35(11)	33(63)	565
$M_4(M_4')$	$L_1 \leftrightarrow L_2 \pm Te \pm TeI$	38(15)	58(68)	450
$M_5(M_5')$	$L_1 \leftrightarrow L_2 \pm TeI \pm TeI_4$	31(16)	62(68)	445

The interesting feature of the As–Te–I system is that there is no immiscibility within the binary border systems. At the same time, there is a wide immiscibility field inside of the ternary system. This field occupies about 60% of the quasi-binary section AsI_3–Te and expands to the both sides, penetrating into the fields of primary crystallization of TeI, TeI_4, C_1 and C_2. Subsequently, some peritectic and eutectic curves pass through this area and transform quadriphase monotectic equilibria (*M_1, M_2, M_3, M_4 and M_5*) (Fig. 6).

The types and coordinates of nonvariant equilibriums are listed in Table 1. Herein, also presented are the invariant equilibriums of binary border systems and quasi-binary sections of the ternary system As–Te–I; degenerate equilibria are marked with the asterisks.

Apparently, our results disagree with the As–As_2Te_3–AsI_3 phase diagram presented in Ref. [6]. Mainly, immiscibility area in a wide composition range was not observed in this subsystem. The section As–$As_4Te_5I_2$ is not quasi-binary and is not characterized by monotectic and eutectic equilibria. In the wide composition range, the liquidus curve belongs to elementary arsenic, which is different from reported in the literature [6] (Fig. 6).

3.1.5. The non-quasi-binary polythermal sections

Figs. 7–10 present some polythermal sections of the phase diagram As–Te–I, clearly representing the processes of the crystallization in the system and also helps to determine the positions of the eutectic, monotectic and peritectic curves.

The section $As_{0.667}Te_{0.333}$–Te (Fig. 7) passes the stoichiometric composition of C_2. Primary crystallization of As (0–42 at.% Te) and Te (50–100 at.% Te) occurs in the wide composition range, while C_1 and α-phase crystallize in a narrow range. The peritectic equilibriums P_1, P_2, P_4, P_5 and P_6 are reflected on this section. The section does not cross the immiscibility field. However, the monotectic eqilibrium M_1 and the three-phase field of $L_1 + L_2 + As$ are observed on the section. The bottom border of the immiscibility field is shown conditionally (dashed line). This section crosses three heterogeneous fields $As + As_2I_4 + C_3$, $As + C_2 + C_3$ and $C_2 + Te$ in the subsolidus region.

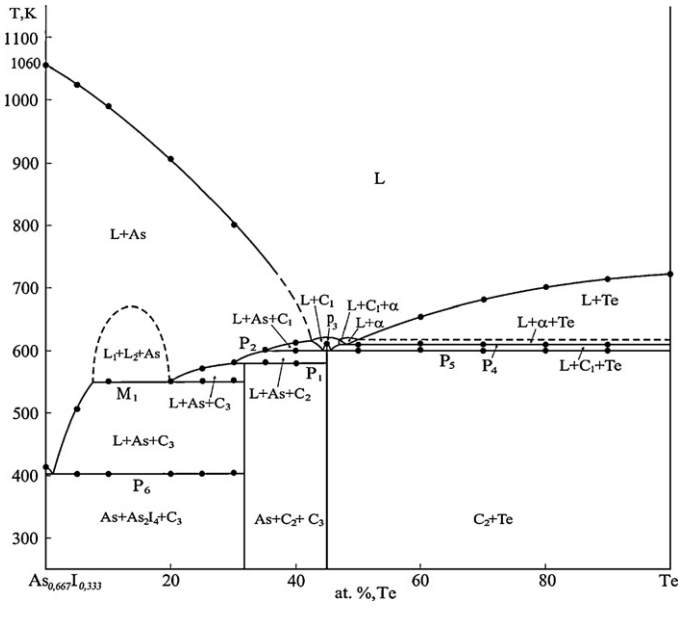

Fig. 7. Polythermal section $As_{0.667}I_{0.333}$–Te of the As–Te–I phase diagram.

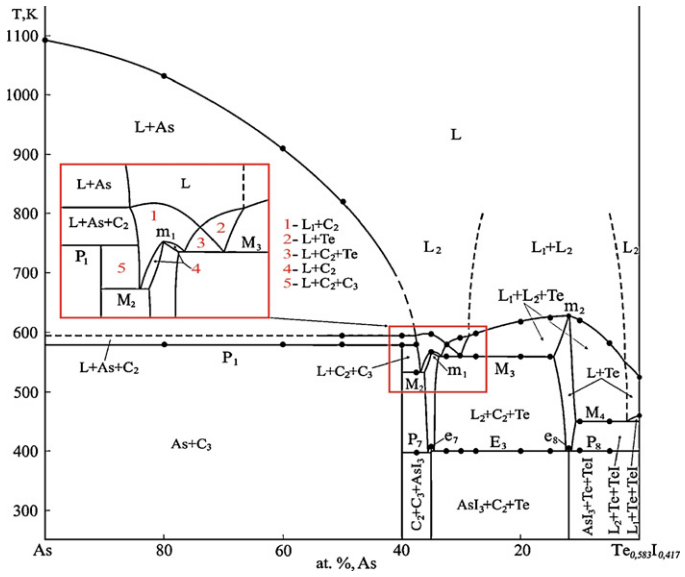

Fig. 8. Polythermal section As–$Te_{0.583}$–$I_{0.417}$ of the As–Te–I phase diagram.

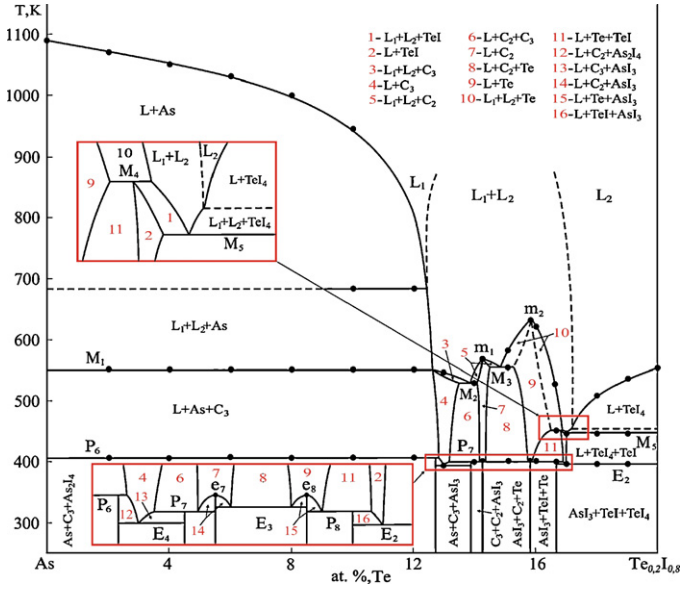

Fig. 9. Polythermal section As–$Te_{0.2}I_{0.8}$ of the As–Te–I phase diagram.

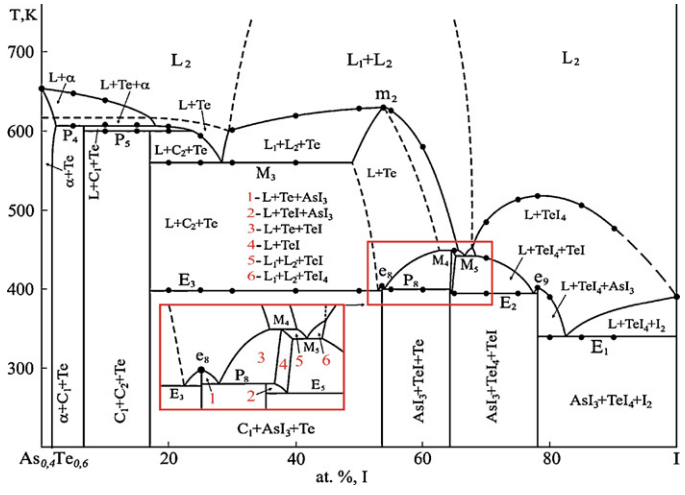

Fig. 10. Polythermal section $As_{0.4}Te_{0.6}$––I of the As–Te–I phase diagram.

Table 2
Temperature dependencies of the EMF for the chains of type (1).

Phase area on Fig. 4	$E = a + bT \pm t\left[\frac{S_E^2}{n} + S_b^2(T-\overline{T})^2\right]^{1/2}$
$C_1 + C_2 + Te$	$E = 66.80 + 0.021T \pm 2\left[\frac{0.24}{25} + 2.4\times10^{-5}(T-360.4)^2\right]^{1/2}$
$AsI_3 + C_2 + Te$	$E = 103.63 + 0.012T \pm 2\left[\frac{0.21}{25} + 2.2\times10^{-5}(T-361.1)^2\right]^{1/2}$
$AsI_3 + C_2 + C_3$	$E = 81.20 - 0.011T \pm 2\left[\frac{0.36}{25} + 3.5\times10^{-5}(T-358.1)^2\right]^{1/2}$

The section $As–Te_{0.583}–I_{0.417}$ (Fig. 8) passes the stoichiometric composition of C_3 (40 at. % As) and the immiscibility fields. This section clearly features some nonvariant equilibria (P_1, M_2, M_3 and M_4) and the curves that connect them. A schematic description of some degenerate non- and monovariant equilibriums and the phase areas around the m_1 are given in Fig. 8 as blow-ups.

The section $As–Te_{0.2}I_{0.8}$ (Fig. 9) crosses six heterogeneous fields in the subsolidus. In the composition area of 12–18 at.% Te, this section is characterized by more complex reaction scheme. A schematic description of some degenerate non- and monovariant equilibriums and phase areas around the m_1 are given in Fig. 9 as blow-ups.

The section $As_{0.4}Te_{0.6}–I$ that crosses three subsystems is shown in Fig. 10 and indicates practically all equilibrium processes in the area As_2Te_3–AsI_3–I–Te. This section crosses the quasi-binary sections AsI_3–Te and AsI_3–TeI_4 at 53 and 78 at. % Te (e_8 and e_9), respectively, and is characterized by the immiscibility area ($L_1 + L_2$) in the region of 29–67.5 at. % Te. Below the solidus, it crosses six heterogeneous fields. Also it helps to precise the positions of the eutectic, monotectic and peritectic curves.

3.2. Thermodynamic functions of arsenic telluroiodides

The EMF measurement results for the chains of type (1) allowed confirming the correctness of all drawn solid-state equilibria and also served as the basis for the calculation of the thermodynamic functions for As_5Te_7I, $As_4Te_5I_2$ and $As_8Te_7I_5$.

The analysis showed the linearity of the EMF dependences upon temperature for various alloys belonging to the heterogeneous fields $C_1 + C_2 + Te$, $AsI_3 + C_2 + Te$ and $AsI_3 + C_2 + C_3$. Accordingly, the linear least-square treatment of the data was performed [18] and the results were expressed according to the literature recommendations [19] as

$$E = a + bT \pm t\left[\frac{S_E^2}{n} + S_b^2(T-\overline{T})^2\right]^{1/2} \quad (2)$$

where n is the number of pairs of E and T values; S_E and S_b are the error variances of the EMF readings and the b coefficient, respectively; $\overline{T}$ is the mean absolute temperature; t is Student's test. At the confidence level of 95% and $n \geq 20$, Student's test is $t \leq 2$ [18]. Using this model (Table 2) and common thermodynamic functions the partial molar functions of arsenic at 298 K were calculated, and the values are shown in Table 3.

According to the phase diagram of the As–Te–I system, the partial molar functions of arsenic in the $C_1 + C_2 + Te$, $AsI_3 + C_2 + Te$ and $AsI_3 + C_2 + C_3$ subsystems are the thermodynamic functions of the

Table 3
Relative partial thermodynamic functions of arsenic in the alloys of the As–Te–I system at 298 K.

Phase area on Fig. 4	$-\Delta\overline{G}_{As}$ (kJ mol^{-1})	$-\Delta\overline{H}_{As}$ (kJ mol^{-1})	$\Delta\overline{S}_{As}$ (J K^{-1} mol^{-1})
$C_1 + C_2 + Te$	21.15 ± 0.19	19.34 ± 1.2	6.08 ± 2.87
$AsI_3 + C_2 + Te$	31.03 ± 0.18	30.00 ± 0.96	3.47 ± 2.73
$AsI_3 + C_2 + C_3$	22.55 ± 0.23	23.50 ± 1.23	−3.18 ± 3.42

Table 4
Standard integral thermodynamic functions of the compounds in the As–Te–I system.

Compounds	$-\Delta_f G^0(298\,K)$ (kJ mol^{-1})	$-\Delta_f H^0(298\,K)$ (kJ mol^{-1})	$S^0(298\,K)$ (J K^{-1} mol^{-1})
AsI_3	65.8 ± 3.2 [21,22]	64.9 ± 3.9 [21,22]	213.1 ± 5.1 [21,22]
As_5Te_7I	137.1 ± 1.4	129.7 ± 5.9	609.4 ± 16.4
$As_4Te_5I_2$	147.3 ± 2,7	143.3 ± 5.8	523.1 ± 13.6
$As_8Te_7I_5$	292.1 ± 6.5	287.4 ± 13.1	942.5 ± 28.5

following potential forming reactions [20]:

$$As(solid) + 0.167As_4Te_5I_2(solid) + 1.5Te(solid) = 0.333As_5Te_7I(solid) \quad (3)$$

$$As(solid) + 0.2AsI_3(solid) + 1.5Te(solid) = 0.3As_4Te_5I_2(solid) \quad (4)$$

$$As(solid) + 0.44AsI_3(solid) + 0.84As_4Te_5I_2(solid) = 0.6As_8Te_7I_5(solid) \quad (5)$$

Using these equations, the integral thermodynamic functions of formation of SbSeI can be calculated as:

$$\Delta_f Z^0(As_5Te_7I) = 3\Delta\overline{Z}_{As} + 0.5\Delta_f Z^0(As_4Te_5I_2) \quad (6)$$

$$\Delta_f Z^0(As_4Te_5I_2) = 3.333\Delta\overline{Z}_{As} + 0.667\Delta_f Z^0(AsI_3) \quad (7)$$

$$\Delta_f Z^0(As_8Te_7I_5) = 1.667\Delta\overline{Z}_{As} + 0.733\Delta_f Z^0(AsI_3) + 1.4\Delta_f Z^0(As_4Te_5I_2), \quad (8)$$

where $\Delta_f Z^0$ are $\Delta_f G^0$ and $\Delta_f H^0$ values for the corresponding compound, and $\overline{\Delta Z}_{As}$ is $\overline{\Delta G}_{As}$, $\overline{\Delta H}_{As}$. For the calculations according to Eqs. (6)–(8), the thermodynamic parameters of AsI_3 were taken from the literature [21,22] (Table 4).

The standard entropy of the ternary compounds was calculated using the following equations:

$$S^0(As_5Te_7I) = 3\Delta\overline{S}(As) + 3S^0(As) + 0.5S^0(As_4Te_5I_2) + 4.5S^0(Te) \quad (9)$$

$$S^0(As_4Te_5I_2) = 3.333\Delta\overline{S}(As) + 3.333S^0(As) + 0.667S^0(AsI_3) + 4.5S^0(Te) \quad (10)$$

$$S^0(As_8Te_7I_5) = 1.667\Delta\overline{S}(As) + 1.667S^0(As) + 0.733S^0(AsI_3) + 1.4S^0(As_4Te_5I_2) \quad (11)$$

For the calculations, the standard entropies of arsenic and tellurium were taken from the database [22] as 36.6 ± 2.2 and 49.5 ± 0.3 J K^{-1} mol^{-1}, respectively. The results of the calculations are presented in Table 4. In all cases the estimated standard deviations were calculated by accumulation of errors.

References

[1] E.I. Gerzanich, V.M. Fridkin, Ferroelectric Materials of Type $A^VB^{VI}C^{VII}$, Nauka, Moscow, 1982.
[2] A. Audzijonis, R. Sereika, R. Žaltauskas, Solid State Commun. 147 (2008) 88–89.
[3] A.V. Shevelkov, Russ. Chem. Rev. 77 (2008) 1–19.
[4] B.G. Korshunov, V.V. Safonov, Halogenide systems, Metallurgy, Moscow, 1984.
[5] A.P. Chernov, S.A. Dembovskii, L.A. Chubirka, Inorg. Mater. 6 (1970) 468–470.
[6] A.P. Chernov, S.A. Dembovskii, N.P. Luzhnaya, Russ. J. Inorg. Chem. 20 (1975) 1208–1212.
[7] A.C. Stergiou, P.J. Rentzeperis, Z. Kristallogr. 172 (1985) 111–119.
[8] R. Kniep, H.D. Reski, Z. Naturforsch. B37 (1982) 151–156.
[9] U. Eggenweiler, E. Keller, V. Kramer, U. Petasch, H. Oppermann, Z. Kristallogr. 214 (1999) 264–270.
[10] V.A. Trifonov, A.V. Shevelkov, E.V. Dikarev, B.A. Popovkin, Russ. J. Inorg. Chem. 42 (1997) 1237–1241.
[11] Z.S. Aliev, M.B. Babanly, Chem. Prob. 4 (2010) 256–259.
[12] M.B. Babanly, Z.S. Aliyev, Yu.M. Shikhiyev, Intern. Conf. High Mater. Technol. Proceedings of Conference, Kiev, 2007.
[13] Z.S. Aliyev, M.B. Babanly, Inorg. Mater. 44 (2008) 1203–1207.
[14] M.B. Babanly, J.C. Tedenac, Z.S. Aliev, D.M. Balitsky, J. Alloys Compd. 481 (2009) 349–353.
[15] R.F. Rolsten, Iodide Metals and Metal Iodides, John Wiley and Sons, New York, 1961.
[16] T.B. Massalski, Binary Alloy Phase Diagrams, Second ed., v.3, ASM Inter Mat. Park, Ohio, 1990, pp. 2242–2244.
[17] A.V. Shevelkov, E.V. Dikarev, R.V. Shpanchenko, B.A. Popovkin, J. Solid State Chem. 114 (1995) 379–395.
[18] K. Doerffel, Statistik in der analytischen Chemie, Grundstoffindustrie, Leipzig, 1990.
[19] A.N. Kornilov, L.B. Stepina, V.A. Sokolov, J. Phys. Chem. 46 (1972) 2975–2979.
[20] M.B. Babanly, Yu.A. Yusibov, V.T. Abishov, EMF method for thermodynamics of the composite semiconductor compounds, BSU pbl., Baku, 1992.
[21] O. Kubaschewski, C.B. Alcock, P.J. Spencer, Materials Thermochemistry, Pergamon Press, Oxford, 1993.
[22] V.S. Yungman (Ed.), Data base of thermal constants of substances. Digital version, 2006, http://www.chem.msu.su/cgi-bin/tkv.